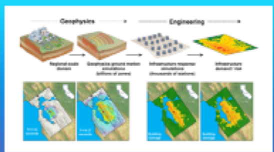

PEER International Pacific Rim Forum
June 16-17, 2021

Quantifying Earthquake Rupture Complexity from Theory and Observations

P. Martin Mai
King Abdullah University of Science and Technology

June 16, 2021

جامعة الملك عبدالله
للعلوم والتقنية
King Abdullah University of
Science and Technology

PEER

Overview

- A quick look ”back into the past”
- Rupture-Complexity Ingredients
  - Spatial variations of on-fault displacement (aka “slip heterogeneity”)
  - Variability of rupture velocity
  - The local slip-rate function: shape & duration
- Constraints from simulations and observations
- Open questions

Early developments

- Earthquake source complexity recognized in the 1960ties and 1970ties
- Omega-square (ω^{-2}) or ω^{-3} model to explain far-field observations (e.g. *Aki, 1967*)
- Theoretical source models developed for point-source like ruptures (e.g. *Brune, 1970*)

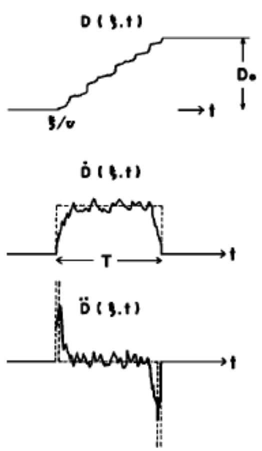

Fig. 1. Schematic diagram of dislocation and its time derivatives at a given point ξ on a fault.

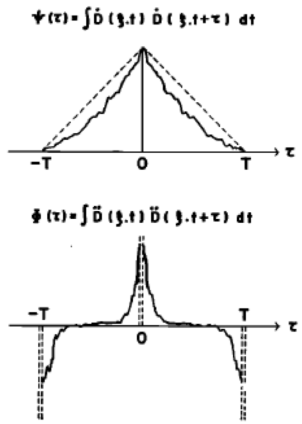

Fig. 2. Schematic diagram of autocorrelation functions of dislocation velocity and dislocation acceleration at a given point ξ on a fault.

Aki, 1967

$$\langle \Omega(\omega) \rangle = \langle \mathcal{R}_{\theta\phi} \rangle \frac{\sigma\beta}{\mu} \frac{r}{R} F(\epsilon) \frac{1}{\omega^2 + \alpha^2}$$

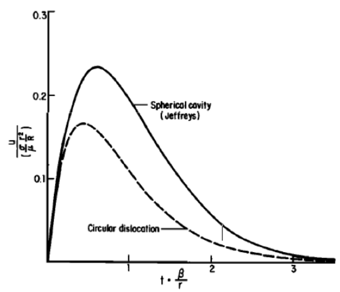

Fig. 4. Comparison of theoretical far-field pulse shapes. Curves for Jeffreys's model of stress pulse on the inside of a sphere and the circular dislocation model developed here shown.

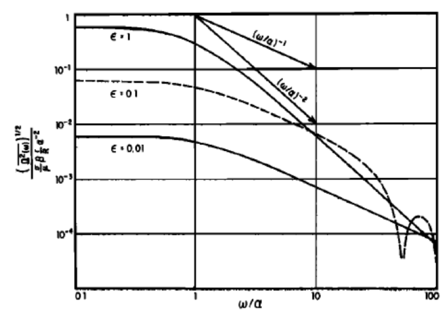

Fig. 5. Average (rms) far-field spectral density curves.

Brune, 1970

1970 1980 1990

Earthquake Rupture Complexity

Early developments

- Extended-fault slip characterization (e.g. *Andrews, 1980, 1981*)
  - Two-dimensional slip function *D(x,z)* with specific properties (in space & FFT domain)
  - Spectral behavior $D(\mathbf{k})$ constrained to $D(\mathbf{k}) \sim \mathbf{k}^{-2}$ by far-field ω^{-2}-decay

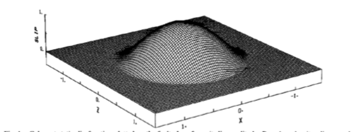

Fig. 1. Coherent static slip function plotted on the fault plane for unit slip amplitude, $D_0 = 1$, and unit radius, $a = 1$.

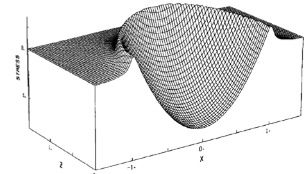

Fig. 2. Coherent static stress change function plotted on the fault plane for $\mu D_0/a = 1$ and $a = 1$.

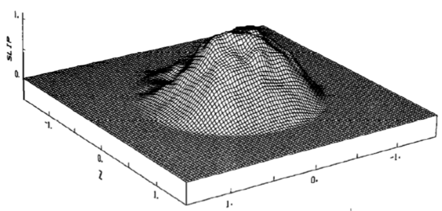

Fig. 3. A realization of stochastic static slip for $D_0 =$

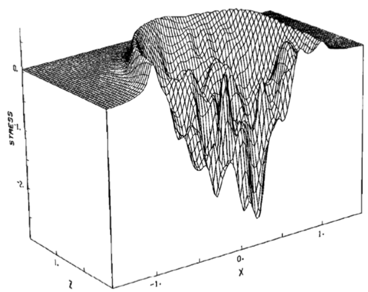

Fig. 4. A realization of stochastic static stress change for $\mu D_0/a = 1$, $a = 1$, and $\nu = 1$.

$$\tau(\mathbf{k}) = K(\mathbf{k}) D(\mathbf{k})$$

$$|D(\mathbf{k})| \propto k^{-\nu-1}$$

$$|\tau(\mathbf{k})| \propto k^{-\nu}$$

$\nu = 1$

$D(\mathbf{k}) \sim 1/\mathbf{k}^2$

"k-square"

$$\tau(\mathbf{x}) = \frac{\mu}{4\pi} \iint \frac{1}{r} \left[\frac{2(\lambda+\mu)}{\lambda+2\mu} D_{,11}(\mathbf{x}') + D_{,33}(\mathbf{x}') \right] dx_1 dx_3$$

$$K(\mathbf{k}) = -\frac{1}{2} \frac{\mu}{k} \left[\frac{2(\lambda+\mu)}{\lambda+2\mu} k_1{}^2 + k_3{}^2 \right]$$

$$k = (k_1{}^2 + k_3{}^2)^{1/2}$$

1970 1980 1990

Early developments

- Apply and extend ideas of *Andrews (1980, 1981)* to earthquake rupture modeling
- Linking spectral decay of far-field displacement to fractal dimension & *b*-values combining many elementary sources (subevents) (*Frankel, 1991*)

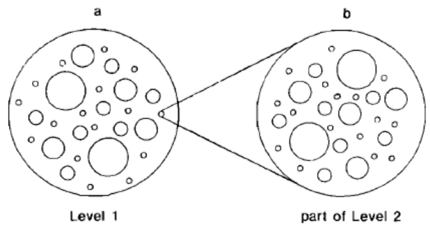

Fig. 1. (*a*) A simplified example of a rupture model with a continuous, self-similar distribution of subevent rupture areas. Rupture zones of subevents are shown by different sizes of circles. The outermost circle represents the rupture area of the main shock. The rupture zones shown in Figure 1*a* are the level 1 subevents. (*b*) A blow-up of one of the subevents in Figure 1*a*, showing that it contains its own self-similar distribution of subevents (level 2).

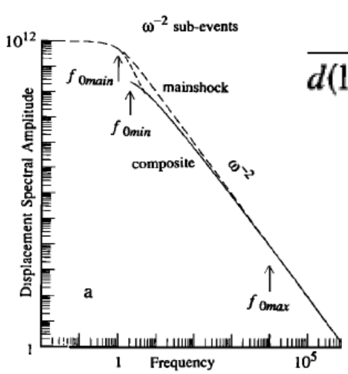

$$\frac{dN}{d(\ln R_{sub})} = p\left(\frac{R_{sub}}{R_{main}}\right)^{-D}$$

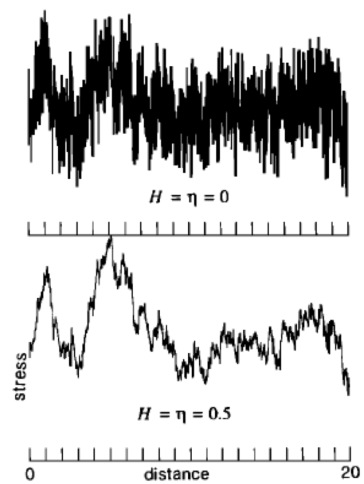

Fig. 6. Two examples of self-similar, random functions representing stress sampled along a line in a fault plane. The top trace has $H = \eta = 0$, a power spectrum proportional to $1/k$ ($D = 2$), and a stress drop independent of scale length. The bottom trace has $H = \eta = 0.5$, a power spectrum proportional to k^{-2}, and a stress drop that decreases with smaller length scales. Distance is given in arbitrary units.

$$\Omega(f) \propto \frac{M_0}{1 + (f/f_0)^{\gamma}}$$

$$M_0 \propto R^{3+\eta}$$

$$\gamma = 3 + \eta - D/2. \qquad (18)$$

Equation (18) indicates that a subevent distribution with $D = 2$ and constant stress drop scaling ($\eta = 0$) will produce a main shock with a falloff of ω^{-2} ($\gamma = 2$) if the subevents fill the main shock rupture area. This is the high-frequency spectral falloff that is typically observed.

1970 1980 1990

Early developments

- Apply and extend ideas of *Andrews (1980, 1981)* to earthquake rupture modeling
- Linking spectral decay of far-field displacement to fractal dimension & *b*-values combining many elementary sources (subevents) (*Frankel, 1991*)
  - Composite source model (*Zeng et al, 1994; Anderson, 2015*)
  - ***k***-square rupture model (*Herrero and Bernard, 1994*)

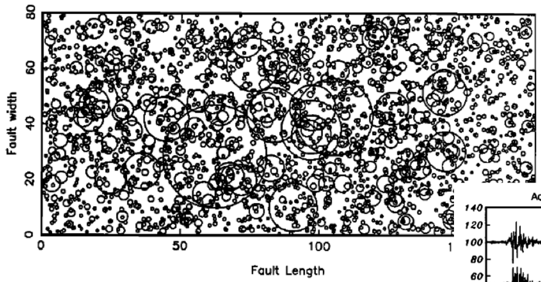

Figure 1. Spatial distribution of 10% of the sube the fault for one simulation.

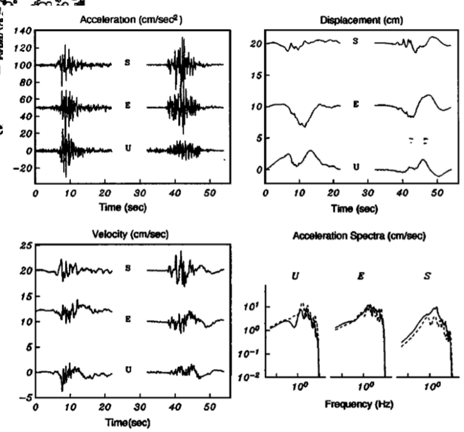

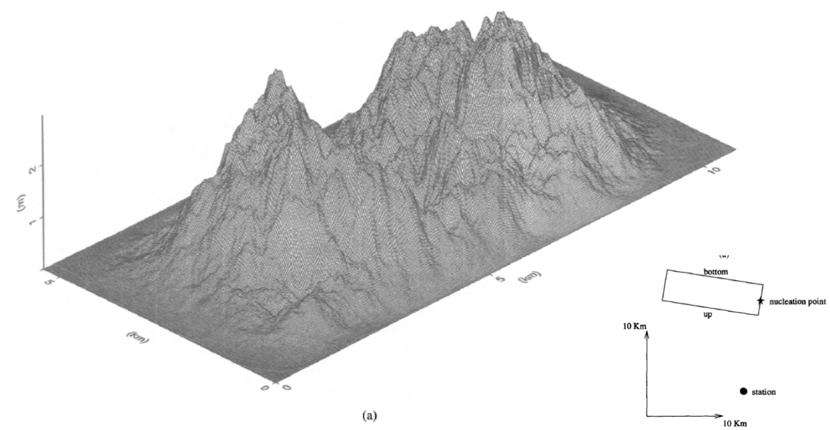

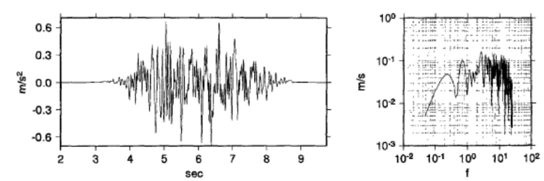

1970 1980 1990

Using finite-fault earthquake source inversion models

- Increasing number of source inversion studies provide “rupture models”
- *Somerville et al (1999)* characterize earthquake slip for 15 such rupture models
  - Processing of 2D slip maps; count asperities (large slip regions); statistical analysis
  - Compare with ***k***-square model

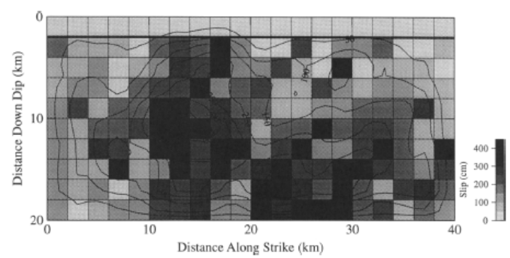

TABLE 7.
Scaling Relations of Slip Models Assuming Self-Similarity

Rupture Area vs. Seismic Moment	$A = 2.23 \times 10^{-15} \times M_o^{2/3}$
Average Slip vs. Seismic Moment	$D = 1.56 \times 10^{-7} \times M_o^{1/3}$
Combined Area of Asperities vs. Seismic Moment	$A_a = 5.00 \times 10^{-16} \times M_o^{2/3}$
Area of Largest Asperity vs. Seismic Moment	$A_l\,(km^2) = 3.64 \times 10^{-16} \times M_o^{2/3}$
Radius of Largest Asperity vs. Seismic Moment	$r_l\,(km) = 1.08 \times 10^{-8} \times M_o^{1/3}$
Average Number of Asperities	2.6
Area of Fault Covered by Asperities	0.22
Average Asperity Slip Contrast	2.01
Hypocentral Distance to Center of Closest Asperity vs. Moment	$R_A = 1.35 \times 10^{-8} \times Mo^{1/3}$
Slip Duration vs. Seismic Moment	$T_R = 2.03 \times 10^{-9} \times Mo^{1/3}$
Corner Spatial Wavenumber Along Strike (km^{-1})	$\log KC_x = 1.72 - 0.5\,M$
Corner Spatial Wavenumber Down Dip (km^{-1})	$\log KC_y = 1.93 - 0.5\,M$

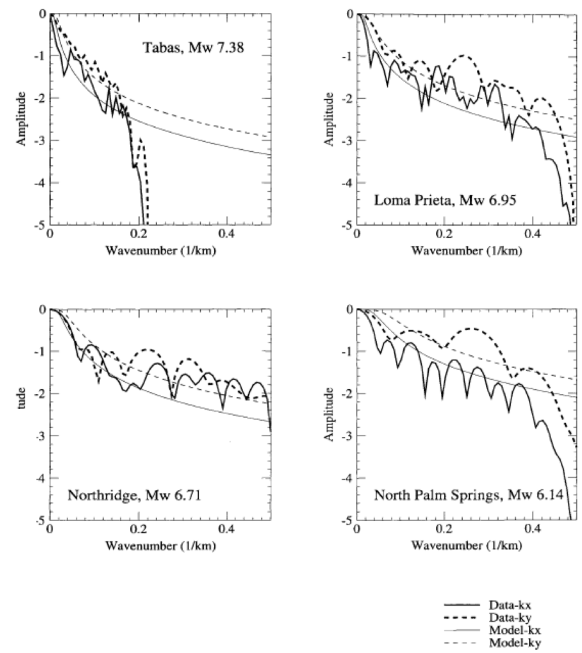

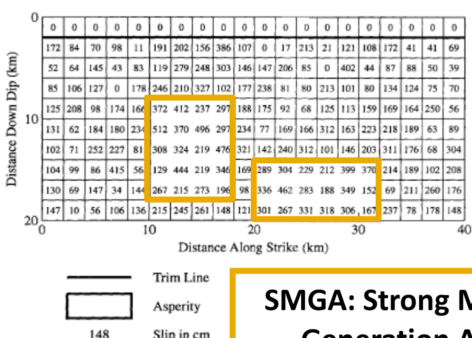

SMGA: Strong Motion Generation Area

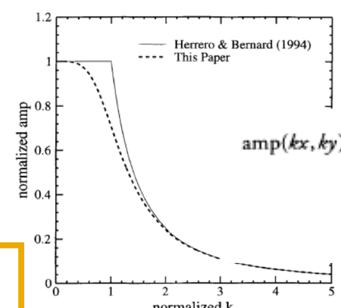

$$\mathrm{amp}(kx, ky) = \frac{1}{\sqrt{1 + \left(\left(\frac{kx}{KC_x}\right)^2 + \left(\frac{ky}{KC_y}\right)^2\right)^{2.0}}}$$

Quantify Slip Heterogeneity

- Compilations of rupture models: fault slip spatially variable
- Slip heterogeneity as spatial random field *(Mai and Beroza, 2002; Lavallee et al, 2006)*
- Use auto-correlation function $C(\mathbf{r})$ in space, or its power-spectral density $P(\mathbf{k})$ in the Fourier domain

	$C(r)$	$P(k)$
GS	e^{-r^2}	$\frac{a_x a_z}{2} e^{-\frac{1}{4}k^2}$
EX	e^{-r}	$\frac{a_x a_z}{(1+k^2)^{\frac{3}{2}}}$
VK	$\frac{G_H(r)}{G_H(0)}$	$\frac{a_x a_z}{(1+k^2)^{H+1}}$

$$G_H(r) = r^H K_H(r)$$

$$r = \sqrt{\frac{x^2}{a_x^2} + \frac{z^2}{a_z^2}}$$

$$k = \sqrt{a_x^2 k_x^2 + a_z^2 k_z^2}$$

$$P(k) \propto \frac{1}{k^{\beta+1}} \propto \frac{1}{(k_x^2 + k_z^2)^{4-D}} \qquad D = E + 1 - H$$

- a_x, a_z: correlation lengths
- H: Hurst number ($H = [0; 1]$)
- K_H: modified Bessel function 2nd kind, order H
- k_x, k_z: wavenumber in horizontal and vertical direction
- fractal: "straight-line" in power-spectral decay,
- fractal dimension D (E: Euclidian norm)

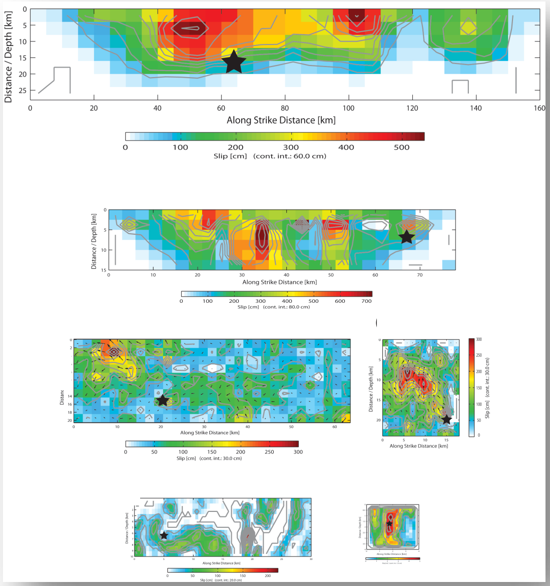

Mai and Beroza, 2002

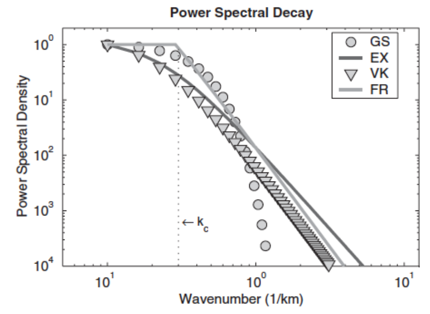

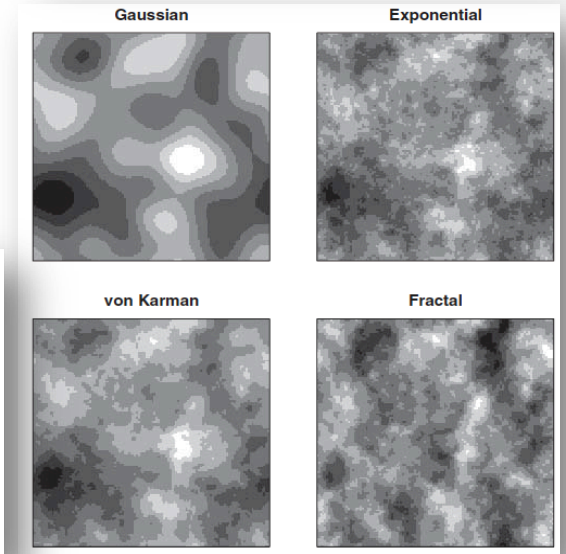

Quantifying Slip Heterogeneity

- Patterns emerging from an analysis of many slip models
  - van Karman ACF best replicates the *P(**k**)* of slip distributions
  - Correlation lengths depend on magnitude
  - Hurst exponent *H ~ 0.7*

$$P(k) = \frac{4\pi H}{K_0(0)} \cdot \frac{a_x a_z}{\left(1+k^2\right)^{H+1}}$$

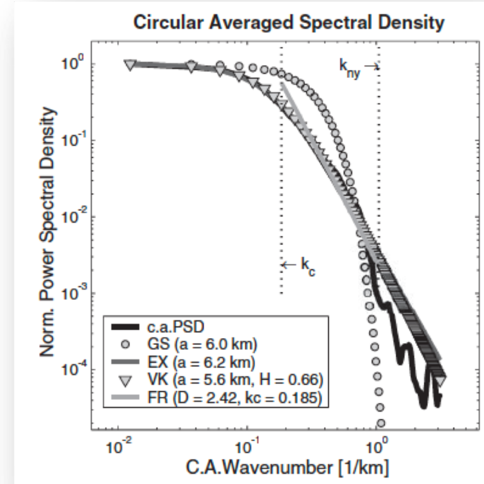

Mai and Beroza, 2002

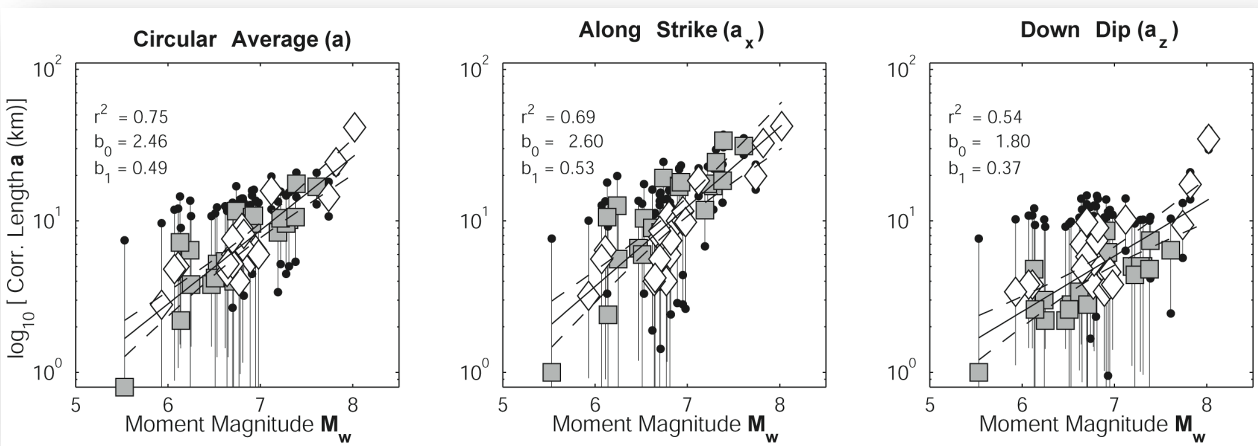

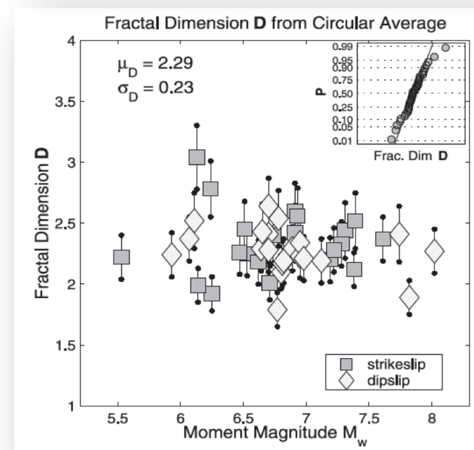

$$a_x \approx 2.0 + \tfrac{1}{3} L_{eff}; \qquad \log(a_x) \approx -2.5 + \tfrac{1}{2} M_w$$

$$a_z \approx 1.0 + \tfrac{1}{3} W_{eff}; \qquad \log(a_z) \approx -1.5 + \tfrac{1}{3} M_w$$

$$D \sim 2.3 \rightarrow H \sim 0.7$$

Earthquake Rupture Complexity

Simulating slip heterogeneity

- For kinematic rupture modeling, tsunami simulations, initial stress for rupture dynamics
  - Assume fault-plane dimensions or calculate from source-scaling relations
  - Simulate "random" but realistic heterogeneous slip distribution
  - Karhunen-Loève expansion (*LeVeque et al, 2016*) for curved faults

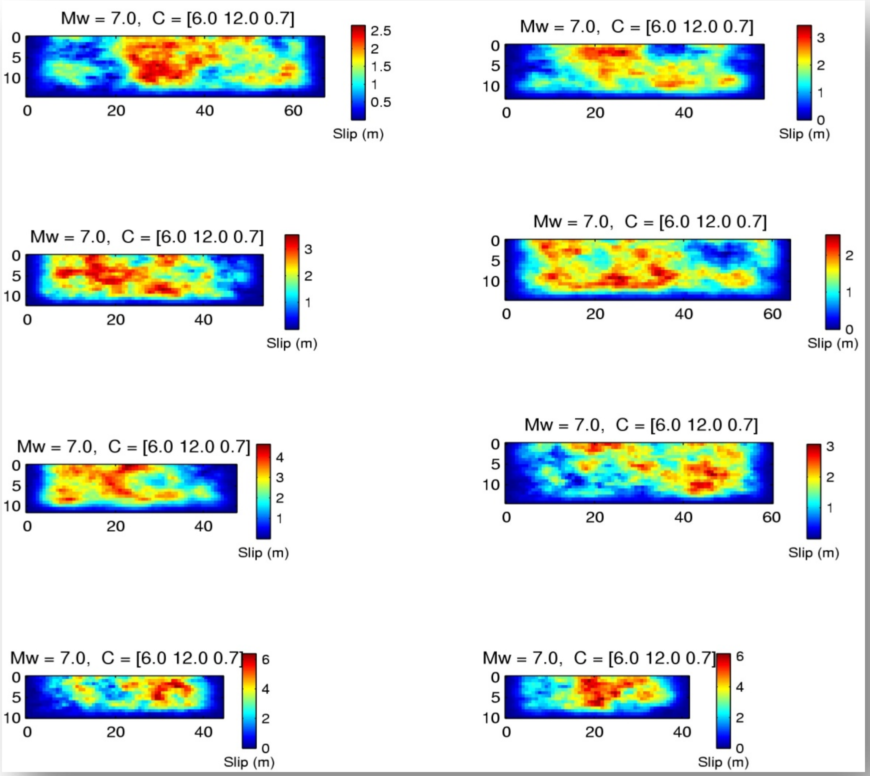

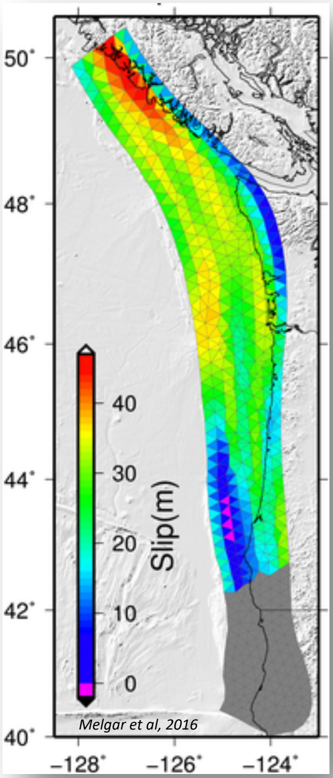

Earthquake Rupture Complexity

Simulating slip heterogeneity & rupture evolution

- Something is missing !
  - Where does the rupture start? → Constrain hypocenter
  - How (fast) does it propagate? → Constrain rupture speed
  - Local slip function on the fault? → Shape, duration, V_{peak}

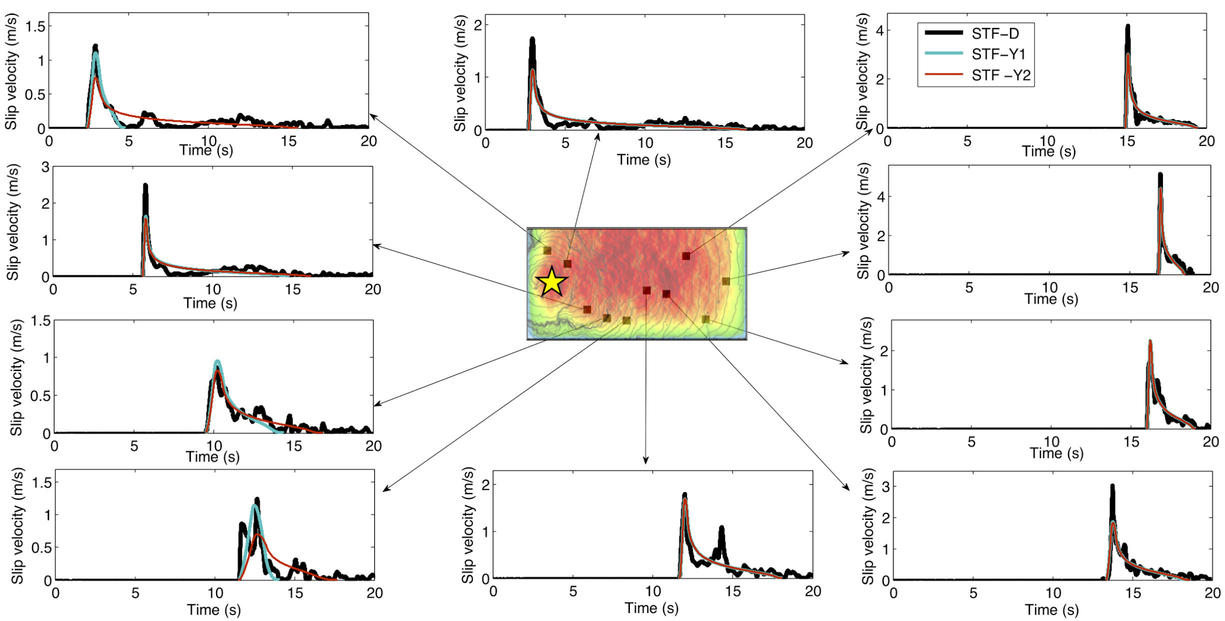

Mai et al, 2018

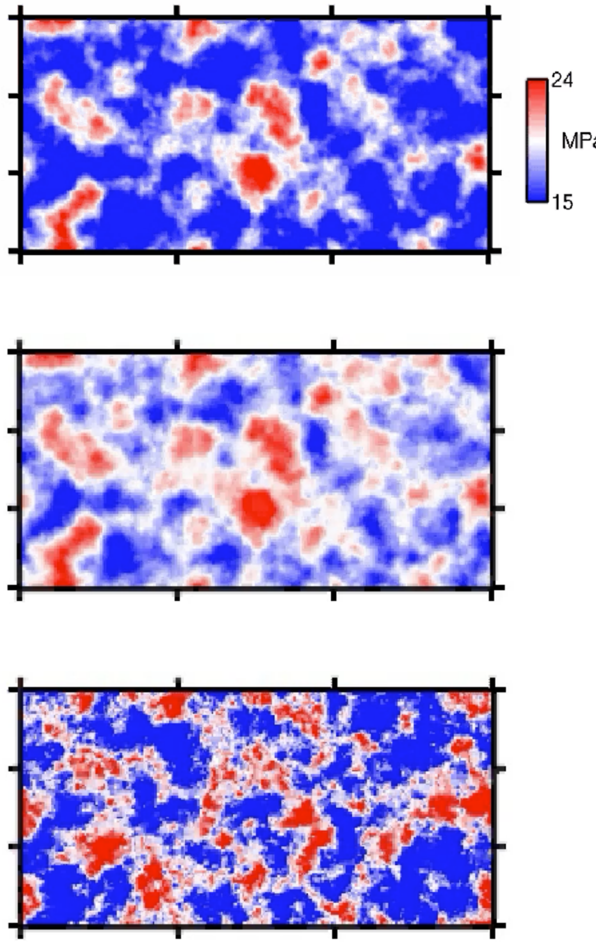

Ripperger et al, 2006

Earthquake Rupture Complexity

Simulating slip heterogeneity & rupture evolution

- **Hypocenter location** – not random, but related to slip (stress) on the fault
- from hypocenter locations in finite-source rupture models
  - ruptures starts on, or close to, a large-slip region (“asperity”)
  - consistent with energy-budget consideration of rupture dynamics
  - ruptures may nucleate at any level of slip

stress change

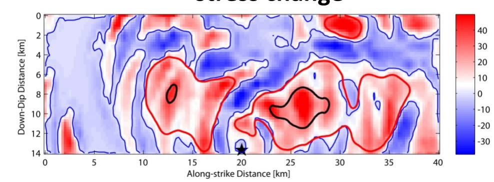

asperity definition

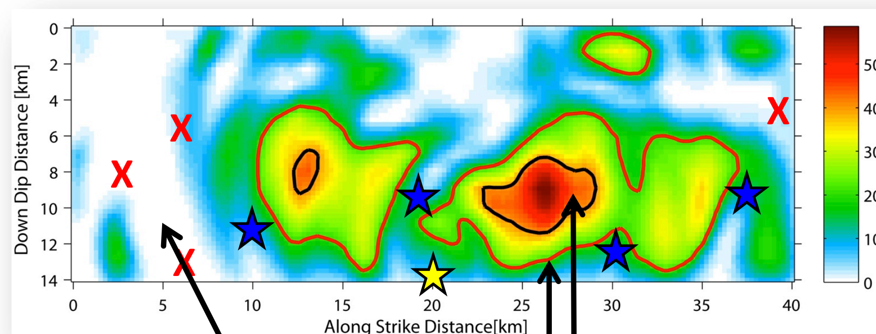

$$D < \frac{1}{3} D_{max}$$

$$\frac{1}{3} D_{max} \leq D < \frac{2}{3} D_{max}$$

$$D \geq \frac{2}{3} D_{max}$$

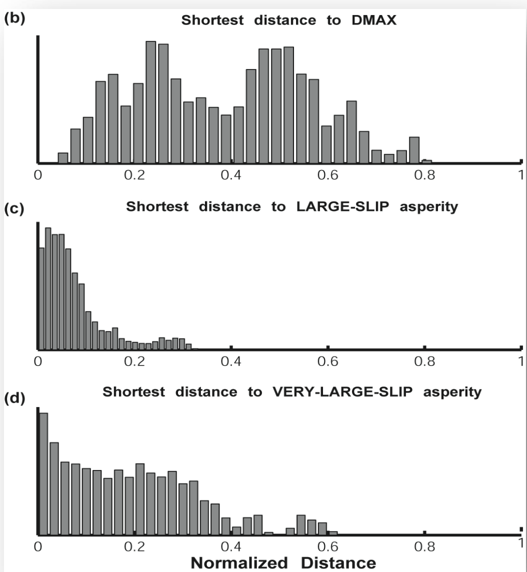

Hypocenter distance w.r.t. zone of large (very-large) slip

Mai et al, 2005

Earthquake Rupture Complexity

Simulating slip heterogeneity & rupture evolution

- **Rupture velocity** can be highly variable over fault plane
  - from finite-fault inversions & dynamic rupture simulations
  - rupture accelerates or slows down locally
  - clearly seen in dynamic rupture simulations
  - conditions for supershear V_r?

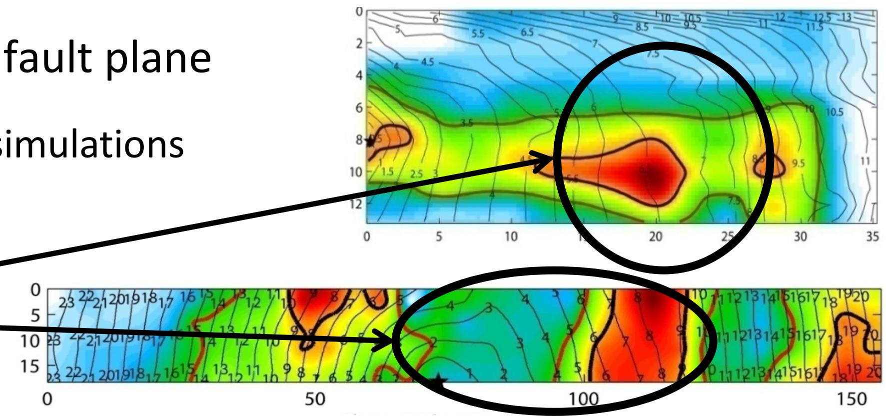

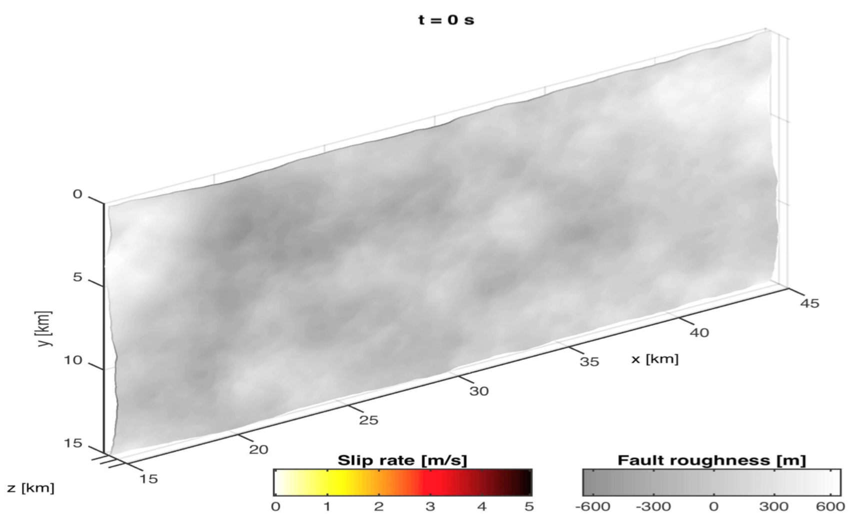

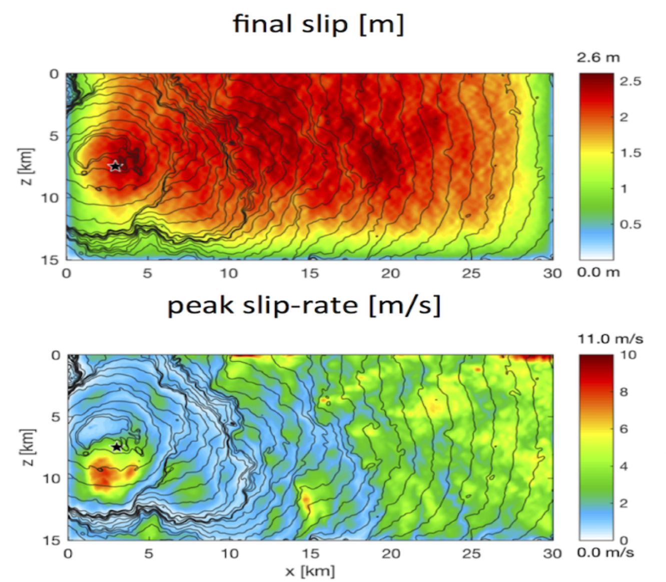

Mai et al, 2018

Simulating slip heterogeneity & rupture evolution

- **Local slip-rate function** (shape, duration, V_{peak}) controls radiation
  - several parameterizations proposed
  - shape, duration (rise time) spatially variable
  - (reg.) Yoffe-type dynamically consistent (*Tinti et al, 2005)*

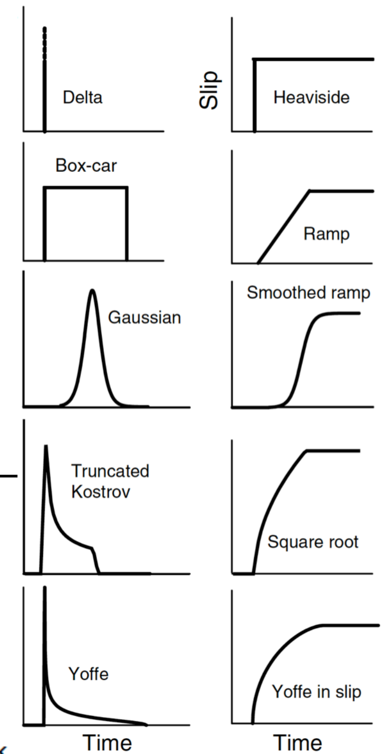

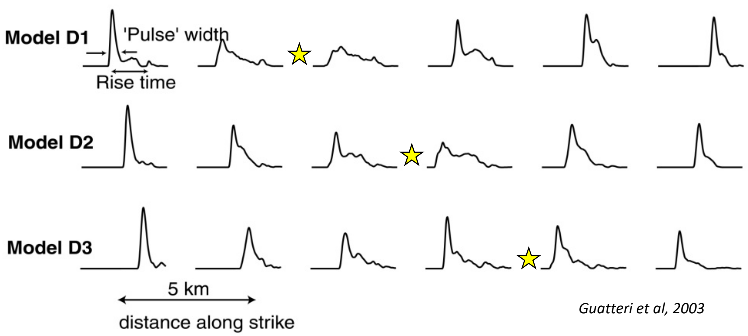

Guatteri et al, 2003

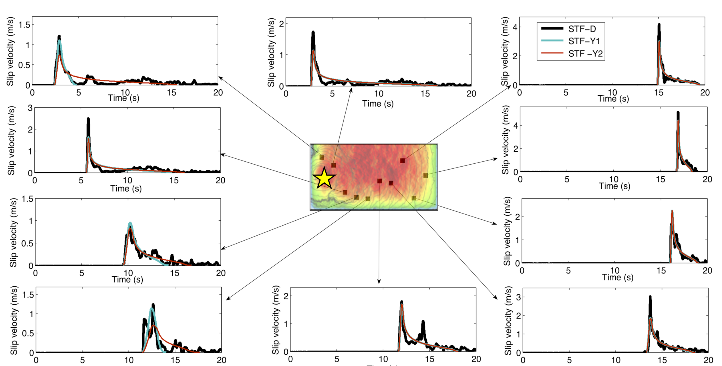

Mai et al, 2017

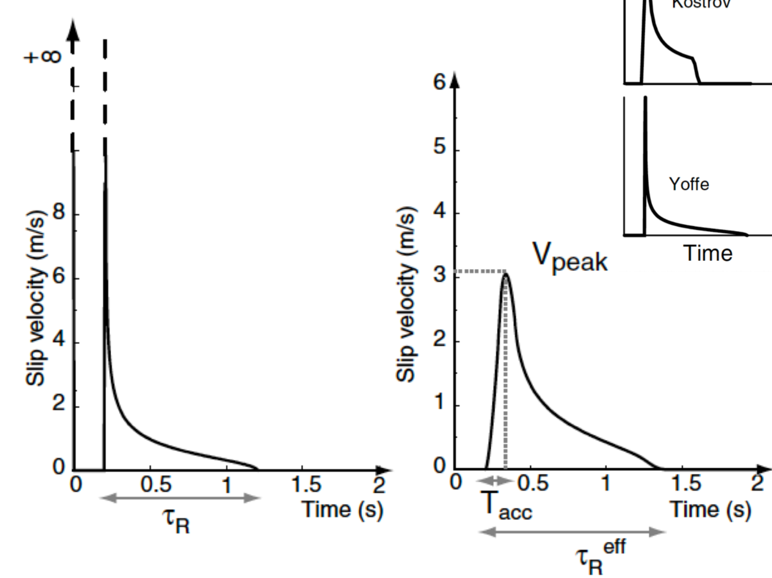

$$V_{peak} = 1.04 \frac{D_{max}}{(T_{acc})^{0.54}(\tau_R)^{0.47}} \simeq C \frac{D_{max}}{\sqrt{T_{acc}}\sqrt{\tau_R}}$$

Tinit et al, 2005

Earthquake Rupture Complexity

Current state of the art in kinematic rupture modeling

- Several (similar) methods in use, with the following work-flow
  - assume/compute source dimension, fault geometry known; define hypocenter
  - generate heterogeneous slip on the fault (perhaps rake-angle variations)
  - constrain rupture propagation V_r: scaling between slip and V_r (*e.g.Guatteri et al, 2003; Schmedes et al, 2010*)
  - constrain rise time τ_r : position on fault and average scaling (*e.g. Guatteri et al, 2003;* Somerville et al. 1999)
  - small-scale random variation from fault roughness *(Graves and Pitarka, 2016; Savane and Olsen, 2020)*

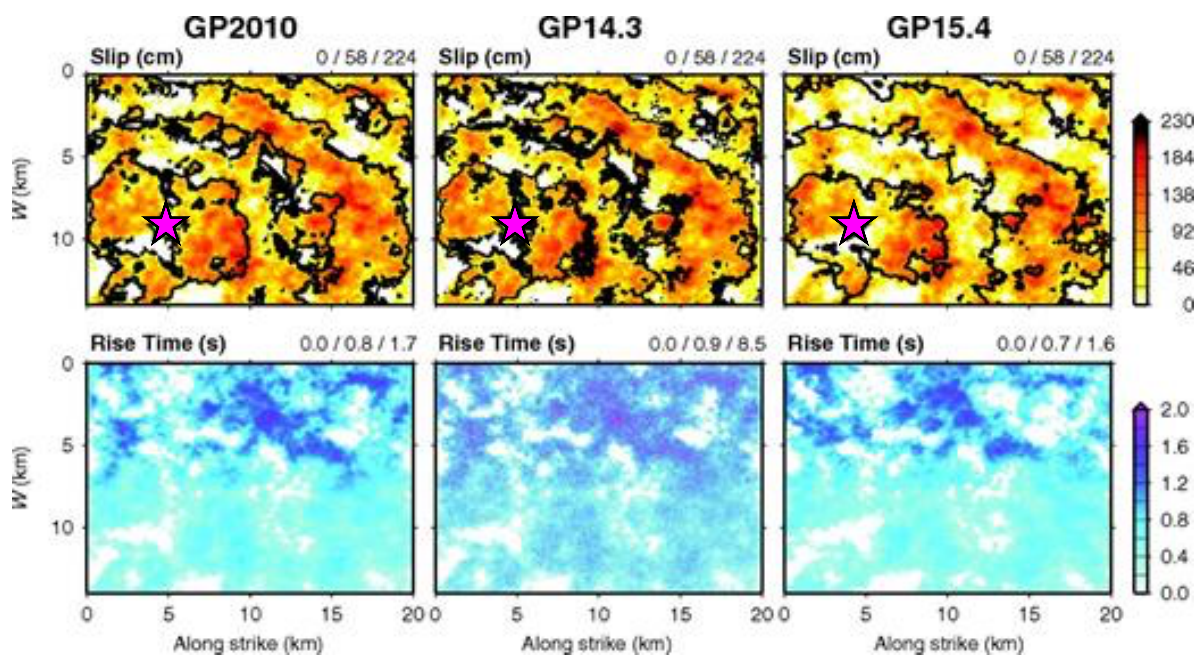

Graves & Pitarka (2006, 2010, 2016)

Open Questions

- Probability distribution of earthquake slip?
  - Non-Gaussian Levy law *(e.g. Lavallee et al, 2006)*; modified log-normal *(Gusev, 2011)*
  - Statistical properties of slip govern ground motions *(e.g., Song and Dalguer, 2013)*
  - Testing probability distributions using SRCMOD database (*Thingbaijam and Mai, 2016*)
  - Evidence for truncated exponential distribution

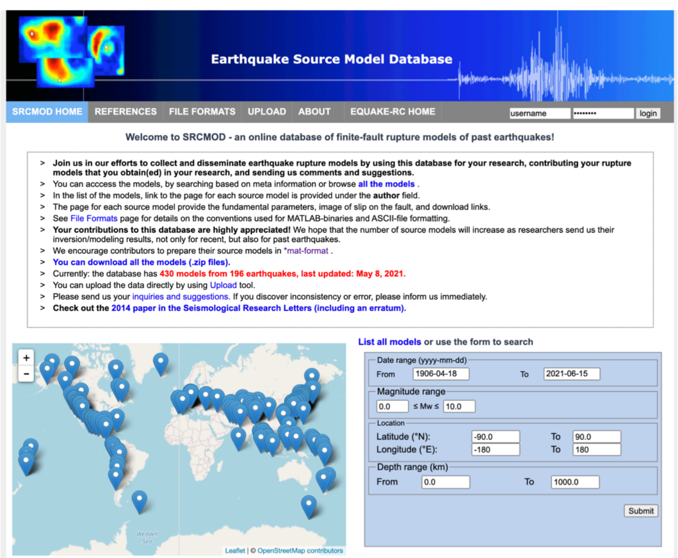

http://equake-rc.info/srcmod
430 rupture models for 196 events (May 2021)

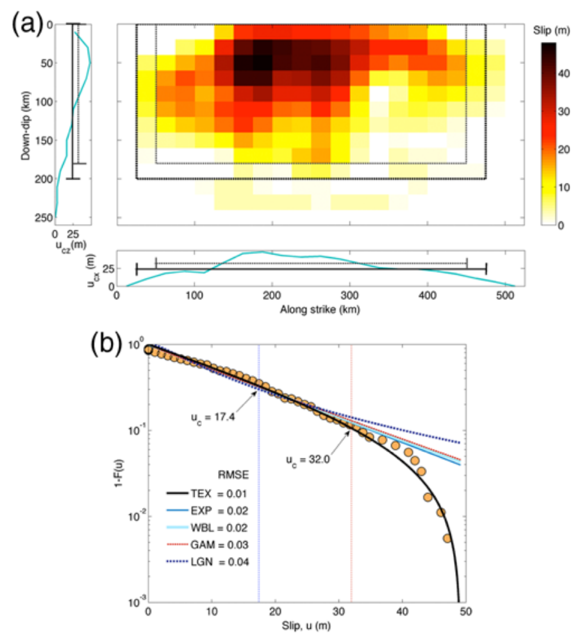

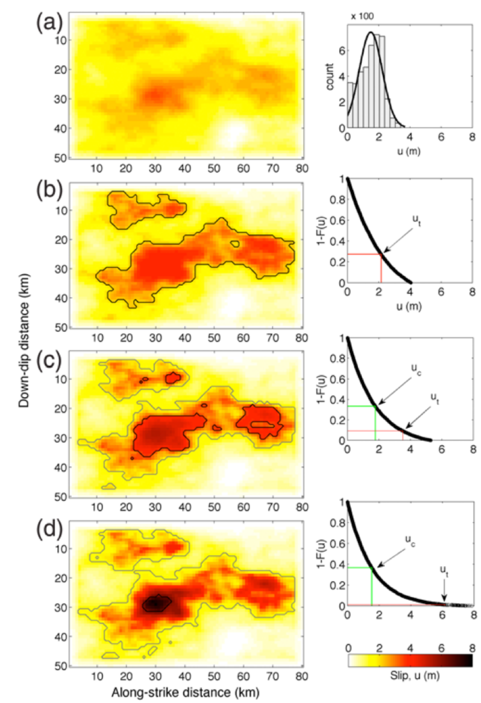

Thingbaijam and Mai, 2016

Earthquake Rupture Complexity

Open Questions

- Intricate rupture dynamics
  - Dynamic triggering, multiple rupture fronts
  - Supershear rupture propagation: episodic and sustained
  - Source-parameter scaling & correlations from dedicated dynamic rupture simulations

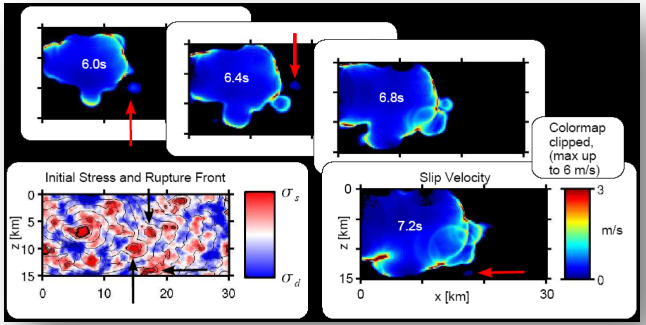

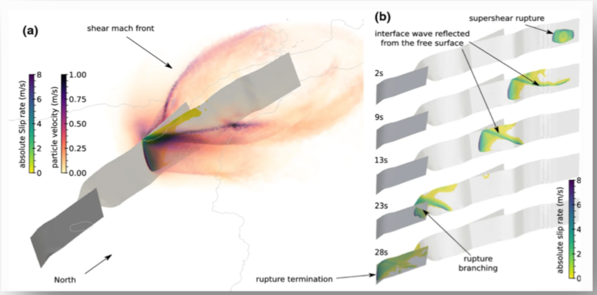

Ulrich et al, 2019

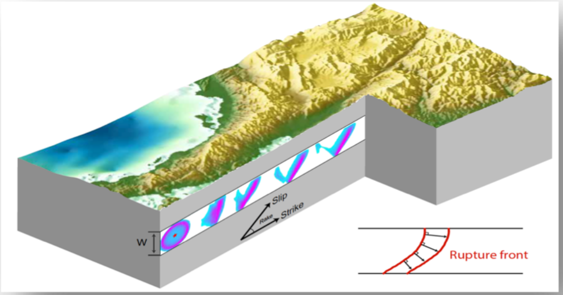

Weng and Ampuero, 2020

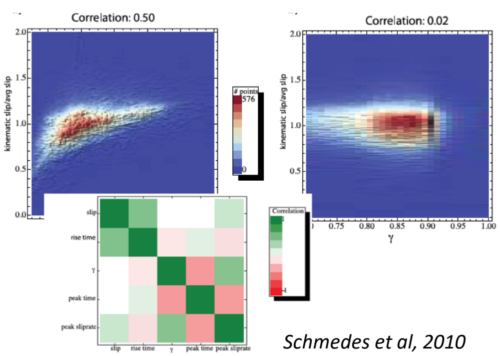

Schmedes et al, 2010

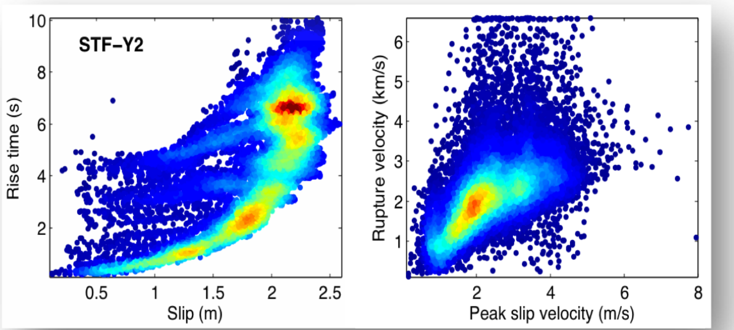

Thingbaijam and Mai, 2016

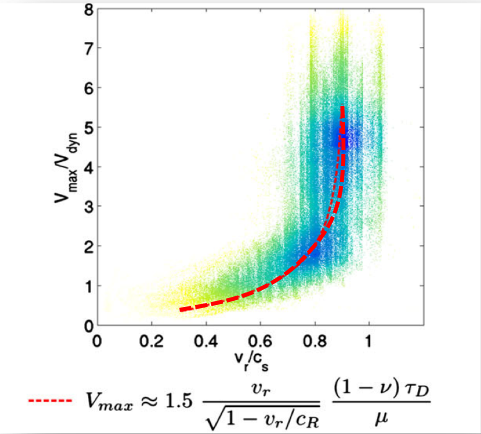

Gabriel et al, 2013

Open Questions

- Compounded multi-segment ruptures
  - Several segments activated in a single (large) event
  - Complex-geometry events require intricate rupture dynamics
  - How to parameterize in a kinematic (pseudo-dynamic) way?

Darfield, NZL (2010)

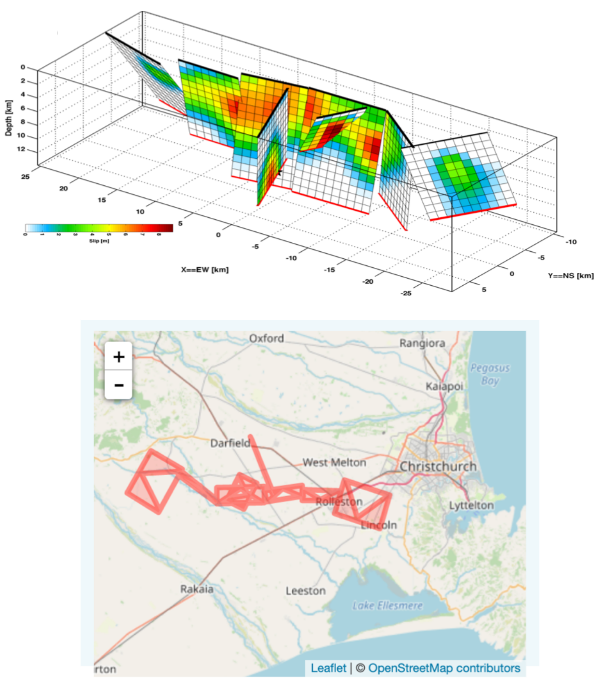

El Mayor Cucapah, MEX (2010)

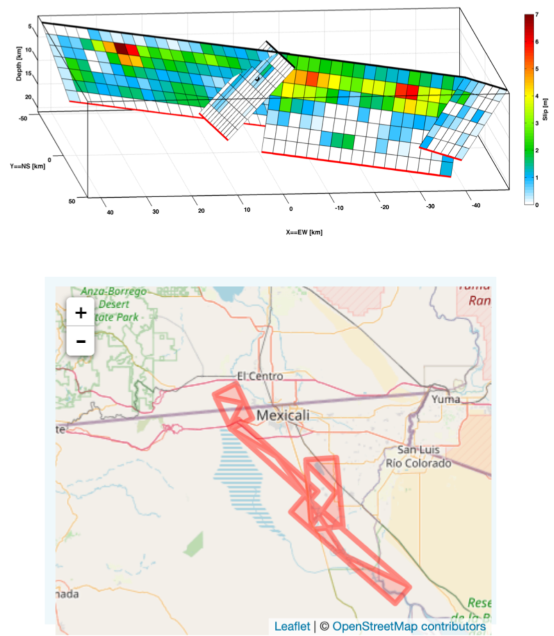

Kaikora, NZL (2018)

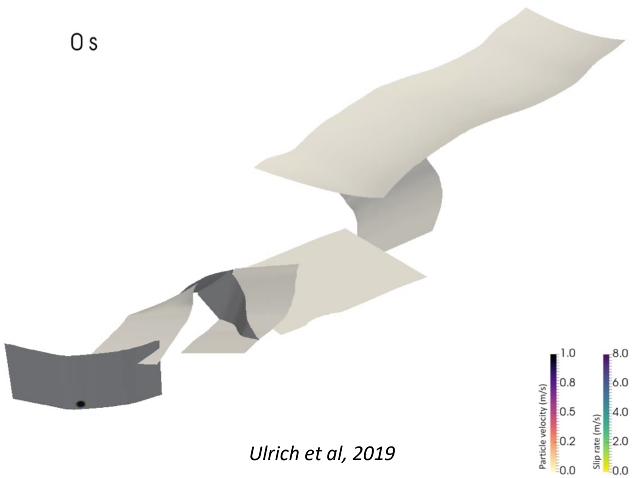

Ulrich et al, 2019

Concluding Remarks

- We have begun to get a handle on imaging & modeling (small-scale) rupture complexity
- Combination of deterministic and stochastic approaches needed to generate the expected high-frequency seismic radiation
- Intricate rupture dynamics only partially accounted for – much more research needed

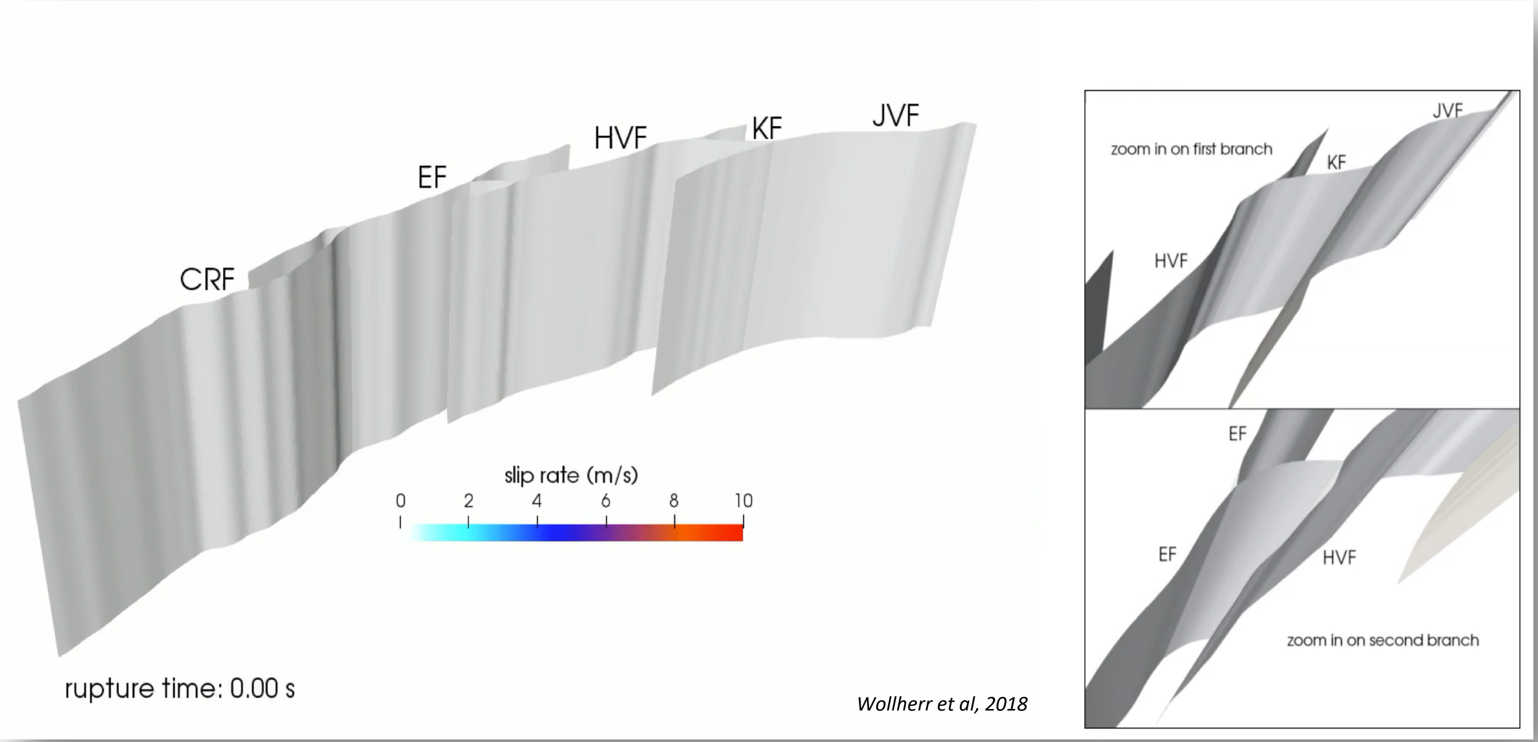

Wollherr et al, 2018

Thank You

martin.mai@kaust.edu.sa